Wide dynamic range APS star tracker

Orly Yadid-Pecht, Christopher Clark, Bedabrata Pain, Craig Staller, and Eric Fossum
Jet Propulsion Laboratory, California Institute of Technology
Pasadena, California, 91109

Abstract

Design considerations and description of a CMOS Active Pixel image sensor (APS) star tracker are reported. APS technology has been thought of being most appropriate for guidance and navigation. However, making APS useful for future star tracker missions means a few challenges have to be overcome. A wider dynamic range is required, while fill factor ought to be high and simple geometry of the pixel active area is desired. These requirements are analyzed and tradeoff considerations are explained for a practical future celestial tracker. A 64x64 element CMOS APS array with individual pixel reset is described.

1. Introduction

Optical tracking has been performed by CCD's for years[1] (Stanton et al.,1987). However, future celestial trackers impose new challenging requirements such as component mass and power consumption reduction, and radiation hardness. Active Pixel Sensor (APS) technology has been proposed as a possible successor for CCD technology[2] (Fossum, 1993a) and has several advantages specifically appealing for star tracker subsystems, i.e. miniaturization, random access, etc. An evaluation of the APS concept for guidance and navigation can be found in recent papers[3,4] (Fossum at al., 1993b and 1994a) and progress in CMOS APS is continually reported.[5, 6,7] (Mendis et al 1993) and (Nixon et al., 1995; Dickinson et al., 1995).

An important requirement for star trackers is a wider dynamic range. Future spacecraft will use images of planets, asteroids as well as stars to make spacecraft control decisions autonomously. This means the star tracker has to have sufficient dynamic range to produce useful images. In some cases there might be as much as 10^8 ratio in brightness between the brightness of a nearby planet and brightest stars[8] (Clark et al., 1995). This need for a wider dynamic range has been recognized a long time ago[9] (McCord and Bosel, 1975). However, an adequate answer has not yet been provided.

Previously suggested solutions for widening the dynamic range could be divided into:
* Compressing the response curve
* Clipping the response curve
* Control over integration time.

Compressing the response curve is done through a sensor with a logarithmic response[10,11,12,13] (Chamberlain, 1984; Caudle, 1985; Mead, 1989; Kub and Anderson, 1993). Clipping is done by some kind of an antiblooming structure[14,15] (Chan, 1984; Decker and Sodini, 1995). Both methods result in loss of detail in the image. The third method mentioned in the literature is controlling the integration time[16,17,18,19] (Komobuchi et al., Chen and Ginosar, Washkurak and Chamberlain, Miyagawa and Kanade, all from 1995). This method has some promising aspects in comparison with others which will be discussed more elaborately in the next section.

The Automatic Wide Accepted Range Detector (AWARD, formerly the Automatic Wide Dynamic Range Sensor) was recently proposed[20,21] (Yadid-Pecht, 1992 and 1993). It consists of a two dimensional array of sensors, each capable of being exposed for a different length of time - autonomously controlled on chip. Autonomous control is a future goal. First step towards it is to provide an APS with local control over integration time, which is the subject of this paper. The chip is referred to as Stracker.

This paper consists of 6 sections. Section 2 covers future star tracker requirements and describes possible options. It also describes previously suggested solutions for controlling the integration time. Section 3 describes the concepts and basic cell design. Section 4 describes the chip architecture and layout. Section 5 describes experimental results. Section 6 concludes the paper.

 0-8194-2028-X/96/$6.00

2. Star tracker requirements and possible options

In this section a list of requirements for the future spacecraft and star tracker system is reviewed. A comparison among possible options like CCD, APS and special APS sensors is given for every required parameter. In the second part previously suggested solutions for local control over integration time will be analyzed.

The list of requirements for the future star tracker system includes:
1. Small size, mass and power consumption
2. Radiation hardness
3. High fill factor
4. High sampling resolution
5. High data rates (windowing)
6. Wide dynamic range

* **Size, mass and power consumption**: The future spacecraft should be smaller, less mass and power. An APS imaging system can reduce power by approximately 100x over CCD systems[22] (Fossum, 1994b). Also, CMOS APS technology allows the integration of timing and control electronics, the imaging array, signal chains and analog to digital converter on the same integrated circuit. This means the number of chips will be reduced, and also circuit board space mass and power consumption. Processes like ADC on chip have already been incorporated in APS and free the system from having additional chips (for opamps, ADC, etc.) solely for this purpose, as in CCD based systems.
* **Radiation hardness**: APS is less sensitive to radiation since charge is not transferred across the array. CCDs are very sensitive to charge transfer efficiency degradation due to proton irradiation.
* **High fill factor**: APS fill factor is approximately the same as the interline CCD (25-30%) and lower than a full frame CCD[22] (Fossum, 1994b).
* **High sampling resolution**: In terms of resolution, number of pixels and pixel pitch, at this stage APS is far behind CCDs. But this will change when the technology is more established.
* **High data rates (windowing)**: APS enables the windowing function, i.e. random access to specific pixels in the image, without the necessity to readout the whole frame. By this, the overall throughput of areas of interest could be higher than in CCD's and high data rates are manageable.
* **Wide dynamic range**: The nature of APS, i.e. being of CMOS technology, enables us to introduce additional features to the sensor. The Stracker project is an attempt to widen the dynamic range of APS sensors, and by such making them suit the star tracker needs and have a relative advantage over other sensor technologies. The method APS Stracker is based on is providing control over integration time which is discussed below.

Table 1 summarizes the requirements for the future star tracker and the advantage of each of the four candidate solutions: CCD, regular APS, and APS Stracker. Three possible attributes have been used, where "❶" designates the best performance in the specified requirement, "❸" is the least and "❷" is medium.

	CCD	*APS*	*APS STRACKER*
Power	❸	❶	❶
Radiation Hardness	❸	❷	❷
Resolution	❶	❷	❷
Fill factor	❶	❷	❷
Windowing	❸	❶	❶
Dynamic range	❷	❷	❶
High Illum. details	❸	❸	❶

Table 1: Summary of Star tracker possible candidate solutions

2a. Control over integration time (external)
External control over integration time, which is the preferred option for APS Stracker at this stage, could be done globally or locally.

Global control over integration time has been achieved via electronic shuttering as well as other means[23] (Cochrun, 1984). This is not satisfactory when a wide dynamic scene is viewed, since part of the sensors might get saturated and white or black patches could be seen in the picture. Specifically, in star trackers, a target can become very bright, as in the case during a close approach to an asteroid or comet nucleus[1] (Stanton et al., 1987). Then, if the brightest pixel contains a full capacity of electrons, other pixels will contain significantly less and will therefore exhibit reduced signal to noise ratios and poorer centroiding accuracy. This means that either the tracker field of view must be sized to assure that the required number of tracked stars all are roughly comparable in magnitude or that other tracker parameters must be chosen so that the degraded centroid/attitude determination accuracy associated with dimmer guide stars is nonetheless sufficient to fulfill the specified pointing requirements[3] (Fossum, 1993b).

Local exposure control attempts have also been made. However, these solutions require a large reduction in fill factor, which is not appropriate to many applications, especially star trackers.
* Matsushita has suggested an IL CCD with Hyper-D-range[16] (Komobuchi et al., 1995). The density of the pixels is doubled, and 8 clock phases are used to produce 2 different exposure times which are superimposed at the readout. For low lights, this sensor will give worse response since the effective area for collection is reduced.
* An adaptive sensitivity CCD image sensor has been suggested[17] (Chen and Ginosar, 1995). It requires an AND gate and a SR flip-flop in each cell, which makes the fill factor very low.
* DALSA has suggested a CCD programmable photodetector where responsivity could be controlled[18] (Washkurak and Chamberlain, 1995). A switched CCD network discards a fraction of the signal charge into a drain and by that increasing the dynamic range.
* In APS technology - interesting work for widening the dynamic range has been carried on in Carnegie Melon University[19] (Miyagawa and Kanade, 1995). However the area of the computational sensor used is around 100μmX100μm and the fill factor is very low.
APS Stracker will be described in the next section.

3. Concept and basic cell description

An image capture pixel includes the sensor, the resetting circuitry and the sampling and readout circuitry. A traditional APS pixel[24] includes a detector, a single reset transistor and readout source-follower circuitry, as shown in Fig. 1a. The detector photogate is labeled PG, the transfer gate TX, the reset transistor RST, and the row selection transistor RS. A photodiode-type APS does not use a photogate, as shown in Fig. 1b, and has been previously described[25]. Since all reset transistor gates in a given row are connected in parallel, the entire row is reset when the reset line is activated. The integration period is the time from pixel reset to pixel readout. In order that pixels on the same row can have different integration periods and do not saturate, individual pixel reset (IPR) is required. Circuitry at the bottom of the column (e.g. load transistor, sample and hold circuitry) is not shown for simplicity, and has been well reported previously[24].

A simple way to implement IPR would be to put a second transistor in series with the row reset transistor, activated by a vertical column reset signal. Unfortunately, this has been shown to introduce reset anomalies when it has been used in CMOS readout circuits for infrared focal-plane arrays for astronomy[26]. This is believed to be due to charge pumping from the output node to the reset drain.

In our work, IPR is implemented via a simple configuration of two reset transistors as illustrated below in Fig. 2. The column reset (CRST) and row reset (RRST) lines must both be at a logical high voltage to activate the reset transistor. While not a major advance in itself, the simple configuration allows low noise, anomaly-free readout, and permits the implementation of a smaller pixel with higher fill factor compared to previously reported efforts for local exposure control[16]. The IPR allows the user to select a small region of interest in the image and adjust the integration time for that region. It is noted that non-destructive readout of the pixel can be performed at any time during the integration period by activating the row select transistor RS and reading the voltage on the column bus. Non-destructive readout can be used to determine the optimum exposure period for a given region of interest.

4. Chip Architecture and layout

The proposed chip has an architecture which is similar to former APS designs. However, to accommodate full random access control, i.e. independent reset and readout per pixel, two sets of row and column controls are provided (Fig. 3). The left and bottom set of row and column decoders are similar to those in former APS designs and are part of the readout control. The top and right set of row and column decoders are provided for independently resetting any pixel address within the array, without interfering with the readout process.

The chip was implemented as an array of 64 x 64 photodiode-type APS elements using the HP 1.2 μm n-well process available through the MOSIS service. The pixel pitch was 20.4 μm (V) x 20.4 μm (H) resulting in a die size of 2.5 mm x 2.6 mm.

Since the modulation transfer function, or MTF, of the sensor is critical for star tracker applications, several different variations of the pixel design was explored. The 64 x 64 element array was divided into 6 regions, each with its own pixel design, as seen in Fig. 4. A L-shaped photodiode pixel (32 x 32 elements) with maximum designed fill factor (28.9%) occupied the upper left portion of the chip. The same pixel with a second level metal light shield covering the entire pixel except the L-shaped photodiode occupied the upper right hand portion of the chip and was also sized at 32x32 elements. A square pixel with a lower designed fill factor (14.6%) occupied a sub array of size 16 x 32 elements. The same pixel but with a light shield covering the entire pixel except the square photodiode occupied the same array size. The fifth design was a rectangular pixel with slightly higher fill factor (15.7%) than the square pixel, and it also occupied a 16 x 32 element subarray, and the same pixel with a light shield like that above occupied the remaining 16x32 element subarray. The expectation was that the L-shaped pixel would have maximum response due to its higher fill factor, but that perhaps the square or rectangular pixels would be easier to use in a centroiding algorithm due to their more regular shape. The light shield helps separate response from the nominally "dead" regions of the pixel containing the readout circuitry from that of the defined photodiode.

5. Test results

The chip was successfully fabricated and tested. The sensor was operated at 5V. Only the RRST signal was driven at 7V to improve the reset of the floating diffusion node. Initial testing focussed on operating the chip in a normal imaging mode, where the total chip readout time was also the integration time. The 64 x 64 element output image was displayed on a monitor using a commercial scan converter. From the visual image, the effect of the light shield was apparent, indicating that significant response is obtained from the "dead" readout region of the pixel. This effect had been previously known from laser spot scanning measurements of intra pixel response.[27]

A second visual observation was that the square pixels without a light shield had the greatest responsivity (volts/watt). The responsivity is related to designed fill-factor, "dead" region response, and capacitance. In general, without dead area response, photodiode-type APS pixels have constant responsivity, independent of pixel size or fill factor. This is because the area of the photodiode contributes both detector area (more responsivity) and capacitance (less responsivity), and these effects cancel. However, the response of the "dead" area increases the signal but does not increase the detector capacitance. Thus, the square pixels, with response in the dead area, had a greater total responsivity.

The sensor was quantitatively tested for relative responsivity, conversion gain, saturation level, input referred noise, dynamic range, dark current and fixed patten noise. The results are presented below in table 2. The conversion gain was in general agreement with the design estimate of capacitance of the photodiode. The saturation level was approximately 2 volts. Read noise of light shielded pixels was typically measured to be higher than that of the non-light shielded pixels, perhaps because the d.c.-biased light shield is capactively coupling in noise to the floating node. The input referred read noise is less than that predicted by simple kTC noise models, as has been observed in other photodiode-type APS arrays. Separate Monte-Carlo modelling work at JPL suggests a reduction of the order of $\sqrt{2}$, a result not far from these experimental results. Fixed pattern noise (FPN), not suppressed by on-chip circuitry, was measured to be approximately 0.5% saturation, or 10 mV peak-to-peak. The FPN results from non-uniformity in the threshold voltages of source-follower circuits at the bottom of each column, since the standard APS sampling of the pixel before and after reset suppresses FPN from pixel-to-pixel threshold variations. Dark current was measured to be of the order of 400-800 pA/cm^2 at room temperature, or 10-20 mV/sec, output referred. A star tracker would typically be cooled to further reduce dark current for longer integration periods. No smear or blooming was observed due to the lateral overflow drain inherent in the APS design.

	Relative response	Conv. gain [µV/e⁻]	Sat. level [V]	Noise [µV] rms	Input ref. noise [e⁻]	Dyn. range [dB]	Dark rate [mV/sec]	Dark rate [e⁻/msec]	Dark rate [nA/cm^2]	FPN
"L" shape	0.74	3.2	1.99	120	38	84	13.6	4.29	0.5	0.45%
Shield. "L"	0.46	3.2	1.91	165	52	81	10.9	3.43	0.4	0.45%
Square	1.00	5.6	1.99	195	35	80	17.7	3.16	0.7	0.45%
Shield. sq.	0.42	4	1.8	205	51	79	15.9	3.97	0.8	0.56%
Rectangular	0.98	4.6	1.99	195	42	80	15.5	3.36	0.7	0.44%
Shield. rect.	0.41	4.6	1.8	225	49	78	16.4	3.56	0.8	0.5%

Table 2. Performance of various sensors.

Functional testing of the pixel resetting circuitry confirmed the operability of the individual pixel reset operation. An area of the chip spanning 16 columns from 16 rows was selected for additional reset. This resulted in a region less-exposed. An output image example is shown in Fig. 5. The darker region of the image represents pixels that were reset during the nominal integration time, so that they had a shorter effective integration time. Some pixels in the majority of the image appear saturated, or white.

The linearity of the "electronic shutter" operation was measured by measuring sensor output as a function of integration time for various exposure settings, but with the same scene illuminance. The output as a function of integration time is shown in Fig. 6. The slopes of these curves are plotted as a function of exposure setting in Fig. 7. The linearity of the electronic shutter is quite good.

6. Conclusions

Future star tracker requirements were examined and analysis of the different possible candidates have been shown. APS Stracker - the first generation APS Star Tracker with wide dynamic range has been described and demonstrated. Stacker gives the future star tracker and APS sensor a potential performance breakthrough and a relative advantage over competing technologies.
Further research should be carried on towards implementing the automatic control of integration time (AWARD) in APS. APS Stracker is the first stage in this effort.

7. Acknowledgements

The authors would like to thank the JPL Advanced Imager Technology Group for their help during various stages of this work, and Mr. Roger Panicacci especially for the help with the layout verification. O.Y-P. appreciates the support of the National Research Council Research Associateship Program.

The research described in this paper was performed by the Center for Space Microelectronics Technology, Jet Propulsion Laboratory, California Institute of Technology, and was jointly sponsored by the Advanced Research Projects Agency, Electronic Systems Technology Office, and the National Aeronautics and Space Administration, Office of Space Access and Technology.

8. References

[1] Stanton R. H., Alexander J. W., Dennison E. W., Glavich T. A., Hovland L. F., "Optical tracking using charge coupled devices", *Optical Engineering*, vol. 26, No. 9, pp. 930-938, Sep. 1987.

[2]Fossum E. R., "Active Pixel Sensors: Are CCD's Dinosaurs?", SPIE vol. 1900, pp. 1-14, 1993a.

[3]Fossum E. R., Bartman R. K., Eisenman A. R., "Application of the active pixel sensor concept to guidance and navigation", SPIE vol. 1949, pp. 1-8, 1993b.

[4]Fossum E. R., "Assessment of image sensor technology for future NASA missions", SPIE vol. 2172, pp. 1-15, 1994a.

[5]Mendis S. K., Kemeny S. E., Gee R. C., Pain B., Kim Q. and Fossum E. R., "Progress in cMos active pixel image sensors", SPIE vol. 2172, pp. 1-11, 1993.

[6]Nixon R. H., Kemeny S. E., Staller C. O., Fossum E. R., "128x128 CMOS Photodiode-type active pixel sensor with on chip timing, control and signal chain electronics", Proc. of the SPIE Vol. 2415, CCD's and Solid-State Optical Sensors V, paper 34 (1995).

[7]Dickinson A., Ackland B., Eid E., Inglis D., Fossum E. R., "A 256x256 CMOS Active Pixel Image Sensor with Motion Detection", ISSCC, Image Sensors and Systems, pp. 256-227, 1995.

[8]Clark C.C., Eisenman A., Udomkesmalee S. and Tubbs E.F., "Application of new technology to future celestial trackers", SPIE Vol. 2446, pp. 100-107, 1995.

[9]McCord T. B. and Bosel J. P., "Potential usefulness of CCD imagers in astronomy", Sym. on CCD for scientific imaging applications, JPL, Caltech, Pasadena, California, pp. 65-69, March 1975.

[10]Chamberlain S.G. and Lee J.P., "Silicon imaging arrays with new photoelements", wide dynamic range and free from blooming", Proc.1984 Custom Integrated Circuits Conf., Rochester, NY, USA, pp. 81-85, 1984.

[11]Caudle D.E., "New generation gated intensified camera", SPIE vol. 569, pp. 107-113, 1985.

[12]Mead C., "Analog VLSI and Neural Networks", Addison Wesley, 1989.

[13]Kub F.J. and Anderson G. W. , "Compressing Photodetectors for Long Optical Pulses using a Lateral Blooming Drain Structure", IEEE Trans Elec. Dev., Vol. 40, No. 10, pp. 1740-1744, October 1993.

[14]Chan T., Barrett O. R., Chen C.W., Abbendini Y., Wen D.D., "A 488x430 Interline Transfer CCD imager with integrated exposure and blooming control", 1984 IEEE Intl. Solid State Circuits Conf., pp. 30-31, San Francisco, CA, 1984.

[15]Decker S. and Sodini C. G., " Comparison of CCD and CMOS Pixels for a Wide Dynamic Range Area Imager", 1995 IEEE Workshop on CCD's and Advanced Image Sensors, Dana Point, California, USA, April 20-22, 1995.

[16]Komobuchi H., Fukumoto A., Yamada T., Matsuda Y. and Kuroda T., "1/4 Inch NTSC Format Hyper-D Range IL-CCD", 1995 IEEE Workshop on CCD's and Advanced Image Sensors, Dana Point, California, USA, April 20-22, 1995.

[17]Chen S. and Ginosar R., "Adaptive sensitivity CCD image sensor", SPIE Vol. 2415, pp. 303-309, 1995.

[18]Washkurak B. and Chamberlain S., "A Switched CCD Electrode Programmable Photodetector", 1995 IEEE Workshop on CCD's and Advanced Image Sensors, Dana Point, California, USA, April 20-22, 1995.

[19]Miyagawa R. and Kanade T., " Integration Time Based Computational Image Sensor", 1995 IEEE Workshop on CCD's and Advanced Image Sensors, Dana Point, California, USA, April 20-22, 1995.

[20]Yadid-Pecht O., "Widening the dynamic range of pictures", in Proc. SPIE/IS&T Sym. on Electronic Imaging: Science and Technology, San Jose, California, SPIE Vol. 1656, High-resolution sensors and hybrid systems, Feb. 9-14, 1992, pp. 374-382.

[21]Yadid-Pecht O., "The Automatic Wide Dynamic Range Sensor (AWDRS)", in 1993 SID Intl. Symp., Seattle, Washington, pp. 495-498, May 1993.

[22]Fossum E. R., "Ultra low power imaging systems using CMOS image sensor technology", Proc. SPIE, Vol. 2267, pp. 107-111, 1994b.

[23]Cochrun B.L., "Linear infrared charged coupled device focal plane with programmable stare time", SPIE vol. 501, pp. 157-163, 1984.

[24]Mendis, S.E. Kemeny and E.R. Fossum, *CMOS active pixel image sensor,* IEEE Trans. Electron Devices, vol. 41(3), pp. 452-453 (1994).

[25]e.g., Yadid-Pecht O., Ginosar R. and Shacham-Diamand Y., *A Random access photodiode array for intelligent image capture,* IEEE Trans. Electron Devices, vol. 38(8), pp. 1772-1781 (1991).

[26]C. Jorquera, C. Beichman, C. Bruce, N. Gautier, and T. Jarrett, *Integration and evaluation of a near infrared camera utilizing a HgCdTe NICMOS3 array for the Mt. Palomar 200-inch observatory,* in Infrared Detectors and Instrumentation, Proc. SPIE vol. 1946, pp. 534-546 (1993).

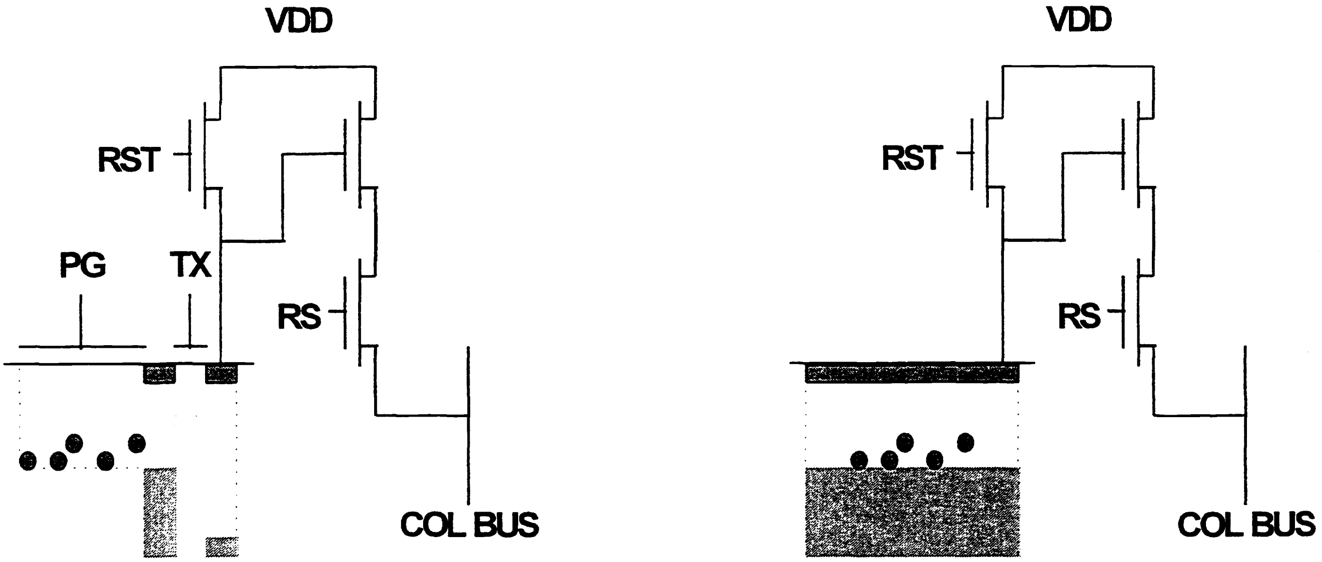

Fig. 1a.(Left) Photogate-type APS pixel circuitry.
Fig. 1b (Right) Photodiode-type APS pixel circuitry.

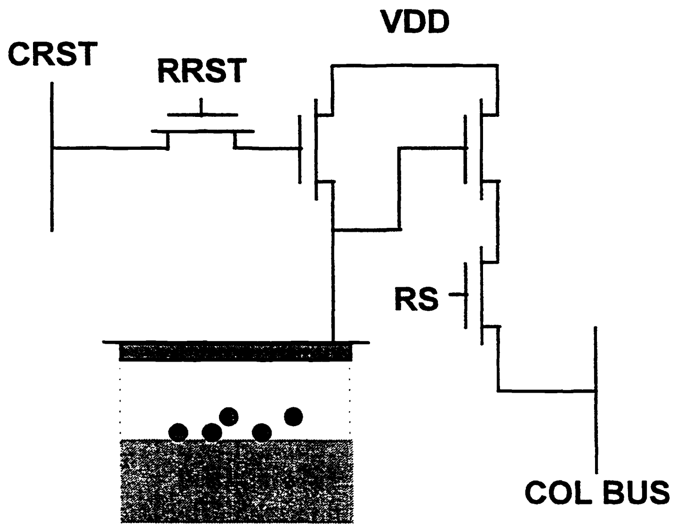

Fig. 2. Photodiode-type APS pixel with individual pixel reset circuitry

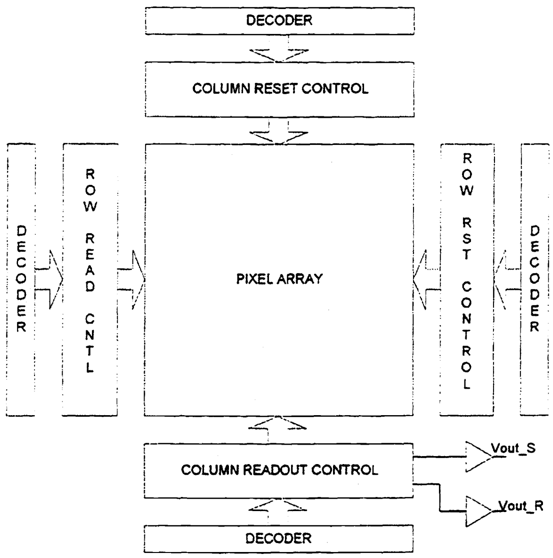

Fig. 3. Block diagram of implemented image sensor

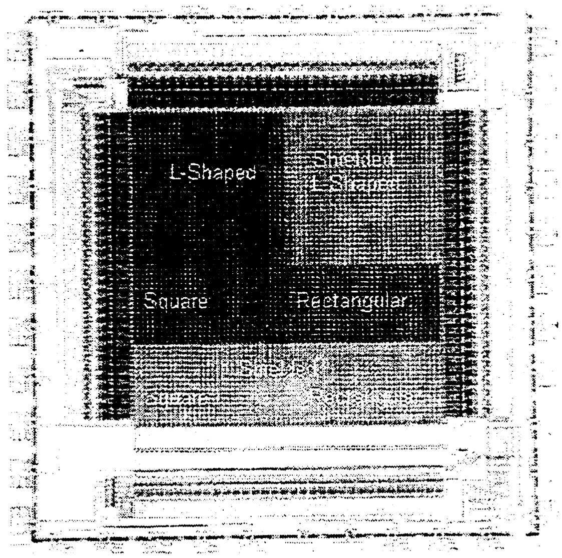

Fig. 4. Photograph of fabricated chip. Labels refer to pixel designs described in the text.

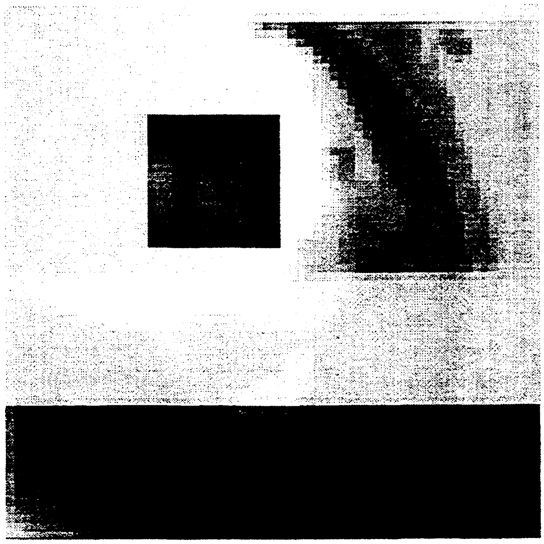

Fig. 5. Sensor output with region of short integration time through George Washington's eye.

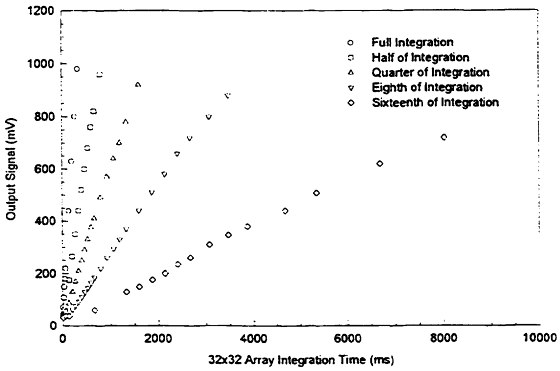

Fig. 6. Sensor output as a function of integration time for various exposure settings.

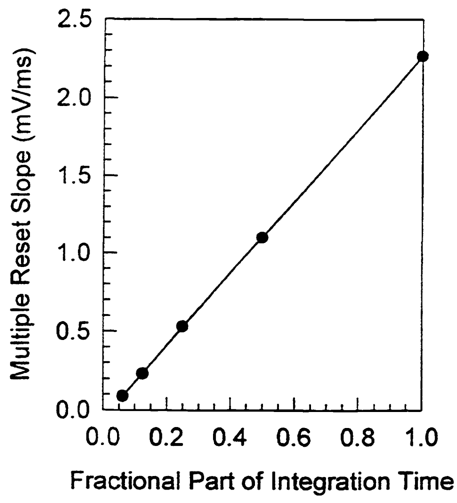

Fig. 7. Linearity of exposure control. Absolute vertical values depend on scene illuminance.